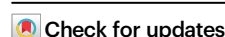


A machine learning and centrifugal microfluidics platform for bedside prediction of sepsis

Received: 11 October 2024

Accepted: 15 April 2025

Published online: 27 May 2025



Lidija Malic^{1,2,3,10}, Peter G. Y. Zhang^{4,10}, Pamela J. Plant^{5,10}, Liviu Clime¹, Christina Nassif¹, Dillon Da Fonte¹, Evan E. Haney⁴, Byeong-Ui Moon¹, Victor Min-Sung Sit¹, Daniel Brassard¹, Maxence Mounier¹, Eryn Churcher⁵, James T. Tsoporis⁵, Reza Falsafi⁶, Manjeet Bains⁶, Andrew Baker⁵, Uriel Trahtemberg^{5,7,8}, Ljuboje Lukic¹, John C. Marshall⁵, Matthias Geissler¹, Robert E. W. Hancock^{4,6}, Teodor Veres^{1,2,9} & Claudia C. dos Santos^{2,4} ✉

Sepsis is a life-threatening organ dysfunction due to a dysfunctional response to infection. Delays in diagnosis have substantial impact on survival. Herein, blood samples from 586 in-house patients with suspected sepsis are used in conjunction with machine learning and cross-validation to define a six-gene expression signature of immune cell reprogramming, termed Sepset, to predict clinical deterioration within the first 24 h (h) of clinical presentation. Prediction accuracy (~90% in early intensive care unit (ICU) and 70% in emergency room patients) is validated in 3178 patients from existing independent cohorts. A RT-PCR-based Sepset detection test shows a 94% sensitivity in 248 patients to predict worsening of the sequential organ failure assessment scores within the first 24 h. A stand-alone centrifugal microfluidic instrument that automates whole-blood Sepset classifier detection is tested, showing a sensitivity of 92%, and specificity of 89% in identifying the risk of clinical deterioration in patients with suspected sepsis.

Sepsis, a complex syndrome of organ dysfunction caused by a dysregulated host response to infection¹, has been declared a global emergency². Estimates from 2017 are >48.9 million cases and 11.0 million deaths per year³, not including deaths from COVID-sepsis⁴. Early individualized interventions^{5,6} may significantly reduce mortality and morbidity, and prevent poor long-term outcomes and disability^{5–7}. It has been shown that even short delays in appropriate treatment can cause significant increases in mortality from sepsis⁷. Despite decades

of research, however, patients are still triaged and treated on the basis of clinical symptoms⁸. While these include measures of overall severity, they are largely nonspecific and do not adequately assess dysregulated responses to infection, align patients with appropriate pharmacotherapies, or predict impending deterioration and the need for resuscitative level care. Biomarkers that provide early prognostic and therapeutic enrichment are actively sought to achieve the personalization necessary to improve research and care^{2,9}.

¹Life Sciences Division, National Research Council of Canada, 75 de Mortagne Boulevard, Boucherville, QC J4B 6Y4, Canada. ²Center for Research and Applications in Fluidic Technologies (CRAFT), University of Toronto, 5 King's College Rd, Toronto, ON M5S 1A8, Canada. ³Department of Biomedical Engineering, McGill University, 775 Rue University, Suite 316, Montreal, QC H3A 2B4, Canada. ⁴Sepset Biosciences Inc., 420 – 730 View St, Victoria, BC V8W 3S2, Canada. ⁵Keenan Research Centre for Biomedical Science, St. Michael's Hospital, University of Toronto, Critical Care Medicine, 30 Bond Street, Toronto, ON M5G 1W8, Canada. ⁶Centre for Microbial Diseases and Immunity Research, University of British Columbia, 232-2259 Lower Mall, Vancouver, BC V6T 1Z4, Canada. ⁷Department of Critical Care, Galilee Medical Center, Nahariya, Israel. ⁸Medicine Faculty, Bar Ilan University, Zafed, Israel. ⁹Department of Mechanical and Industrial Engineering, University of Toronto, 5 King's College Road, Toronto, ON M5S 3G8, Canada. ¹⁰These authors contributed equally: Lidija Malic, Peter G. Y. Zhang, Pamela J. Plant. ✉e-mail: Claudia.santos@utoronto.ca

Early diagnosis of sepsis is critical to favorable outcomes⁷. Currently sepsis diagnostic methods include pathogen detection (using conventional or real-time multiplex PCR methods), clinical algorithms based on various tests and risk factors in the patient medical records, biomarkers including procalcitonin (PCT), C-Reactive Protein (CRP), lactate, white blood cell shape (Intellisep test) and a variety of proposed markers (Calprotectin, MCP-1, Presepsin, etc.)⁹. The proposed international gold standard sequential organ failure assessment (SOFA) score and its early analog quick SOFA (qSOFA), and more recently a host response molecular test termed Septicyte have also been studied^{10,11}. Unfortunately, at first clinical presentation, these tests have poor ability to identify patients at risk of developing sepsis.

Importantly, while some diagnostic tests have moved to a ‘distributed’ model with relevant tests performed at bedside (e.g., glucose monitoring for diabetes), for patients with sepsis, the vast majority of biochemical and molecular tests are implemented in a ‘centralized’ format, found only in well-equipped laboratories that require trained operators and specialized instruments, making them less accessible (or even inaccessible) to some of our most vulnerable and difficult to access populations^{8,12–14}. The need to send samples to the lab for analysis significantly delays results (some more than the 6 h recommended by the surviving sepsis guidelines)¹⁵ and limits the ability to provide timely care to patients^{6,16,17}. This ‘bottleneck’ means that testing standards fail one of the primary objectives of the World Health Organization (WHO) “to promote health, ...and serve the vulnerable so everyone, everywhere can attain the highest level of health.”¹⁸

Lab-on-a-chip (LOC)^{19–22} technologies have the potential to advance care beyond traditional ‘syndromic’ approaches, outside specialized centers, promising to democratize care for millions of patients^{23–25}. In addition to performing assays in a compact, miniaturized format, LOC devices promote portability and point-of-care (POC) testing, enabling minimally trained personnel to perform analytical procedures outside laboratory settings. We have previously shown that extraction and detection of molecular markers from biological samples, such as blood, can be fully automated using a centrifugal-based LOC system²⁶. We have further integrated bioanalytical assays for pathogen detection involving polymerase chain reaction (PCR)²⁷ and loop-mediated isothermal amplification in a sample-to-answer format²⁸. Combining our LOC system with innovative RNA-based biomarkers that predict clinical deterioration^{29–33} may significantly advance sepsis care in specialized and non-specialized settings alike.

In parallel, our group discovered and validated a 99 gene signature, present within 2 h of presentation to the emergency department (ED), able to predict clinical deterioration based on the emergence of a cellular reprogramming profile, associated with the inability of cells to respond to pathogens^{34,35}. Our original expression signature was pathogen agnostic, predicting both all-cause and COVID sepsis and different immunological response endotypes. The signature was also predictive of organ dysfunction and severity outcomes^{33,36}.

Here, we hypothesize that a reduced gene signature, can discriminate patients with suspected sepsis at high risk of clinical deterioration. We validate the ability of the signature to classify patients into two deterioration risk groups, defined by a worsening sequential organ failure assessment (SOFA) score, as per Sepsis-3 definitions of sepsis, using our own independent cohort through quantitative real-time reverse transcriptase polymerase chain reaction (qRT-PCR, N=248). We further validate the quantitative molecular assay with digital droplet PCR (ddPCR) to detect the RNA-based Sepset classifier at the POC using our centrifugal microfluidic system, termed the PREcision mEDicine for CRITICAL care (PREDICT) device, which predicts whether patients will go on to develop sepsis in <3 h using 50 μ L of whole blood (N=30) in the near-patient environment.

Results

A high-level overview of the risk prediction classifier, platform development path and deployment workflow is shown in Fig. 1. Three groups of independent cohorts (Supplementary Table 1) were used to reduce our original 99-gene signature down to 6 genes. We then validated, in a blinded fashion, the classifier’s ability to accurately identify amongst 248 well characterized patients, those who went on to deteriorate clinically, as defined by worsening of the sequential organ failure assessment (SOFA ≥ 2) score and the need for ICU admission, 24 h post-initial assessment (early for patients with prospective sepsis).

Our own whole blood RNA sequencing (RNA seq) data from 586 samples from 514 individuals (176 ICU and 338 ER patients); including 392 previously published³³ and 194 new patient samples, were used to refine the gene expression signature able to predict clinical deterioration in patients with suspected sepsis^{33,34,37}. Briefly, these data were generated from whole blood tubes collected from consenting adult patients (>18 years of age) with ethics approval, who presented with prospective sepsis, within the first 2 h of emergency room (ER) or

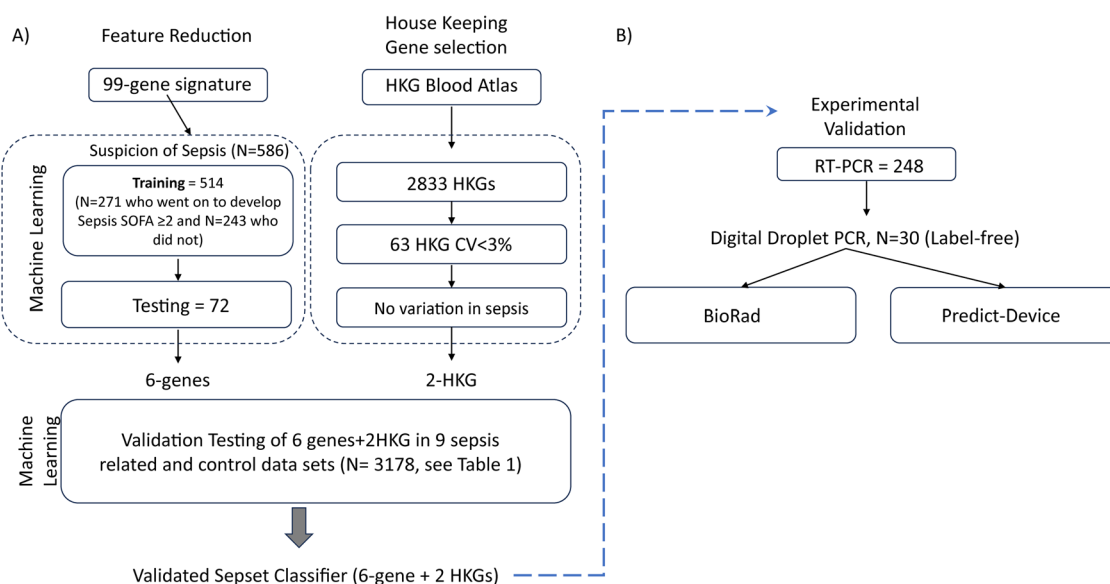


Fig. 1 | Overview of prediction classifier development, validation and analytical performance testing. A Machine Learning, feature reduction and validation of the Sepset classifier. **B** Experimental Validation and Analytical Performance Testing of the Sepset Classifier on the PREDICT device.

Table 1 | Summary Performance for Sepset signature and classifier

RNA-Seq Dataset	AUC	Sensitivity	Specificity	Precision	NPV	Accuracy	Reference
COVID-19 Sepsis (N = 359)	0.85	85%	72%	85%	71%	79%	An ³⁹
ICU Validation (N = 176) ^a	0.9	92%	82%	88%	88%	87%	This study
ER Validation (N = 338) ^a	0.69	70%	59%	63%	67%	65%	This study
Scicluna (N = 802)	0.99	97%	90%	99%	61%	94%	Scicluna ²⁹
Davenport (N = 371)	0.83	86%	62%	59%	88%	74%	Davenport ³²
Burnham (N = 327)	0.92	87%	83%	74%	92%	85%	Burnham ⁶²
Kalantar (N = 152)	0.81	83%	65%	61%	86%	74%	Kalantar ⁶³
McClain (N = 201)	0.96	92%	91%	58%	99%	91%	McClain ^{64,65}
Tsalik (N = 280)	0.86	75%	88%	70%	91%	82%	Tsalik ⁶⁶
Pankla (N = 138)	0.97	94%	100%	100%	92%	97%	Pankla ⁶⁷
Arunachalam (N = 34)	0.89	83%	95%	91%	91%	89%	Arunachalam ⁶⁸
Aggregated Data (N = 3178)	0.88	87%	78%	80%	83%	83%	
Negative Control Data Sets							
Stage 3/4 Cancer (n = 1755)	0.5	0%	100%	-	63%	50%	TCGA/GDC ⁶⁹
Cardiogenic shock (n = 33)	0.53	0%	100%	-	52%	50%	Yang 2022 ⁷⁰
Coronary Artery Disease (N = 353) ^b	0.51	3%	100%	100%	51%	51%	McCaffrey ⁷¹
Inflammatory Bowel Disease (N = 1030) ^c	0.53	0%	100%	-	21%	51%	Argmann ⁷²
Bacterial infection (N = 170) ^b	0.39	83%	9%	38%	43%	46%	Smith ⁷³
Viral infection (N = 64) ^c	0.48	0%	93%	0%	83%	46%	Dapat ⁷⁴

Performance of the Sepset signature was evaluated in different validation and testing datasets comprised of transcriptomic analyses of samples collected from various regions and settings. Aggregated results include analysis of patient samples subjected to transcriptomic analysis and available in the literature (see specific references). The internal data sets, samples indicated as “This Study”, were from an independent subset of patients from the Biomarkers of Lung Injury study (ClinicalTrials.gov ID NCT04747782), a prospective, observational, clinical study that collected whole blood from patients who presented to the ICU or ward with acute respiratory distress and suspected sepsis. All datasets are publicly available Supplementary Table 1. Definitions: NPV Negative Predictive Value, ICU intensive care unit, ER emergency room.

^a These datasets were distinct subsets of the training set and performance criteria might be affected by overfitting.

^b McCaffrey⁷¹; 353 patients with coronary artery disease comparing 189 positives (MID/MID + /CAD) to 164 negatives (LOW CAD).

^c Argmann⁷²; comparing 819 inactive/Mild/Moderate/Severe IBD blood-based transcriptomes to 211 healthy controls.

within 24 h of intensive care unit (ICU) admission (see Methods) as previously published^{33,34,37}.

Each of the previously published 99 cellular reprogramming signature genes³³ was tested for their ability to discriminate between 271 patients with suspected infections who went on to record a SOFA score >2 in the first 24 h of presentation and the 243 who did not. We used 514 first samples (out of total of 586) for machine learning (ML) model training and the remaining 72 second samples (out of 586) from the same 514 individuals as well as samples from 50 healthy individuals as validation samples. We selected six upregulated genes with the highest specificity, fold-change (FC) and lowest adjusted *p*-value (adj *p*-value, Supplementary Table 2). Increased FCs were associated with eventual worsening of SOFA scores as demonstrated in Supplementary Fig. 1A showing the relative expression values for each of the putative signature genes as a function of the 24-hr SOFA score. This revealed a relationship between the relative gene expression of each signature gene and SOFA score ($p < 0.01$ to $p < 0.0001$). Supplementary Fig. 2B, shows no relationship between lactate level and increased SOFA scores in sepsis samples (SOFA ≥ 2) vs. non-sepsis samples (SOFA < 2). Scattering of expression values around the mean implied that no single gene was discriminatory on its own, justifying the need for a multi-gene risk-prediction expression signature. The six-gene signature arose from the larger immune dysfunction (cellular reprogramming) signature³⁴. Genes comprising the signature and their abbreviated putative biological functions are shown in Supplementary Table 3.

To ensure we did not need to include positive and negative controls in the prognostic assay, the expression of each of our 6 genes was compared to two housekeeping genes (HKG) selected from the list of the 2833 HKGs expressed in blood cells³⁸. Their expression variance (coefficient of variation, CV) was analyzed in the entire data set and 63 genes showing CV < 3% across all of our datasets were selected as

candidate HKG. These were filtered for lack of variance according to the clinical metadata considering sex, age, SOFA score, location (ICU vs ER), sepsis mortality, prediction and endotype³³, as well as lack of variance in cancer patients (Table 1 and S1). The accuracy of prediction using ratios of individual genes to HKG was tested. While no single gene expression ratio can discriminate those patients that are imminently at risk of clinical deterioration from those that are not, the collective set of 6 genes, when compared to 2 HKGs, gave excellent performance (Table 1).

To determine the best ML model to predict clinical deterioration within the first 24 h following clinical presentation, the input transcriptomic and associated clinical outcome data were analyzed using an ensemble of ML approaches. In patients with suspected sepsis, a SOFA cut-off score of 2 was used to discriminate sepsis from non-sepsis⁴. Using a change of SOFA score of >2 did not substantially change the results. Groups of patients were analyzed in a binary fashion (prospective sepsis cf. non-sepsis), using 18 machine learning algorithms, initially adopting a 10X cross-validation strategy. We chose to proceed with eXtreme Gradient Boosting (XGBoost) (<https://xgboost.ai/>), a regularizing gradient boosting framework/library involving matrices of decision trees, since it gave us the best performance (Table 1 and Supplementary Fig. 2). Negative control data sets were used to reduce the likelihood of identifying false positives - patients with non-septic pro-inflammatory, shock, malignancy and infectious (bacterial or virus non-septic) conditions.

A six-gene signature classified patients with sepsis in independent cohorts and was robust over time and a range of disease severity

We determined the ability of the six-gene compared to two-HKGs signature to accurately classify patients into pre-specified sepsis

groups using nine sepsis-related gene expression datasets ($N = 3178$ (all samples) – 514 (training, or ICU + ER) = 2664) downloaded from the Gene Expression Omnibus (GEO) repository. In these independent external cohorts, the reduced signature was able to discriminate between septic versus non-septic patients (Sepsis-3 criteria¹), with a sensitivity ranging from 83–97% and balanced accuracy of 74–94%, a combined mean sensitivity of 85%, a specificity of 76%, and an accuracy of 81% (Table 1). We then analyzed samples from patients that were seen in the ER with suspicion of sepsis ($N = 338$) versus those admitted directly to the ICU from the training cohort ($N = 176$); this yielded sensitivity assessments of 70% and 92% respectively³³. To determine if the signature was robust over time and a range of disease severity, we assessed its performance in a validation cohort from the Biobanque Québécoise de la COVID-19 (BQC-19; Quebec COVID-19 Biobank) comprised of 359 blood samples taken at various times from 133 patients hospitalized with COVID-sepsis and exhibiting a range of severity^{36,39}. The ability of the reduced signature to discriminate between samples from patients that went on to clinically deteriorate (increased SOFA > 2 or ICU admission) within the first 24 h from initial assessment, compared to those that did not was very good, with sensitivity and balanced accuracy of 85% and 79%, respectively. The set of six genes and two HKGs comprising the signature, we called here Sepset, was able to discriminate patients with suspicion of sepsis at risk of clinical deterioration.

Sepset RNA amplification using RT-PCR reliably identifies patients that clinically deteriorated 24 h after initial assessment

To validate changes in gene expression using RT-PCR, we designed sets of PCR primers that spanned intron-exon boundaries (i.e., only contained in RNA not DNA), that amplified specific regions for each of the mRNA isoforms selected by the ML analysis ($> 90\%$ of mRNAs), avoiding common single nucleotide polymorphisms (SNPs), for each of the 6 signature and 2 HKGs. Control experiments demonstrated that our primers successfully amplified mRNAs of interest extracted from human blood in an RNA copy number dependent manner, amplified as few as 10–20 copies of the gene and gave Ct curves in < 25 cycles with blood mRNA. The PCR primers were then combined in triplex reactions and tested using whole blood RNA extracts from healthy donors. Reaction efficiencies were 100% with as little as 0.2 ng of input RNA (Supplementary Fig. 3). We then tested the Sepset signature in a blinded fashion, using label-free whole blood samples from our in-house cohort of patients with prospective sepsis not included in the training set. As shown in Table 1, in 248 patients, Sepset was able to identify patients who went on to deteriorate with worsening SOFA score (fulfilling sepsis diagnosis based on SOFA ≥ 2 and suspicion of infection) within the first 24 h after sampling for RT-qPCR analysis, to those who did not. In these independent samples, Sepset demonstrated an AUC of 0.88 and a sensitivity of 94%.

Association between Sepset with clinical features of clinical deterioration 24 h after initial assessment

In 248 patients, we looked at the association between presence of Sepset with demographic characteristics, clinical features of sepsis, severity, and outcome measures at baseline, at 24 h (day 1) and 72 h (day 3) post-initial assessment (Supplementary Table 4). In the first 24 h, the signature was correlated with the number of comorbidities, SOFA score, the use of antibiotics, mechanical ventilation, and fluid resuscitation, but not oxygen or vasopressor therapy. Interestingly, we found no association with specific clinical parameters of organ dysfunction until day 3 (72 h) post-initial assessment. At 72 h, culture positivity and 28-day mortality correlated with the presence of the signature. At both 24 h and 72 h post-initial assessment, the signature was associated with important clinical outcome parameters such as the need for ICU admission, initiation of mechanical ventilation, use of fluid resuscitation, and initiation of antibiotics, as well as outcome

parameters such as ICU length of stay. Unfortunately, we did not have data on dialysis requirements, but while presence of urine output at baseline was not associated, an increase in serum creatinine correlated with Sepset expression.

Digital droplet PCR detected the Sepset classifier in 0.5 ng of patient-derived whole blood RNA

To migrate precision RNA-mark detection onto the LOC device, we designed the microfluidic platform to measure RNA expression using ddPCR. Herein, primers that spanned exon-exon junctions, were designed for each of the 8 genes (6 Sepset and 2 HKG) in the signature. The performance of each primer was benchmarked using the Bio-Rad AutoDG/QX200 reader. Serial dilutions of human cDNA plasmids obtained from the mammalian genome collection⁴⁰ were used to determine limits of detection (1 copy/ μ l) and dynamic range of the probes for each of the genes of interest (Supplementary Fig. 4A left panel). Verification of primer performance was conducted using universal human cDNA (Supplementary Fig. 4A middle panel) and 500 pg of patient cDNA (Supplementary Fig. 4A right panels). A total of 500 pg of patient cDNA resulted in optimized partitioning of the positive and negative droplets and quantitation of the Sepset signature.

We then established the conditions for multiplexing using FAM and HEX labeled probes at final concentration of 5 μ M (Supplementary Fig. 4B left panel). Representative 2D tracing (Supplementary Fig. 4B bottom right panel) showed partitioning of double negative (bottom left quadrant), FAM only (upper left quadrant), HEX only (lower right quadrant) and double positive (upper right quadrant) droplets. Probes alone (no cDNA) as a control rendered only double negative droplets (bottom right panel). Counts (in copies/ μ L) for each gene were obtained in triplicate and used to further refine the training of the predictive algorithm. Primers and probes used for ddPCR are presented in Supplementary Table 5.

PREDICT platform detected the Sepset classifier at the point-of-need

Having validated the ability of the Sepset classifier to identify patients with ‘prospective’ sepsis, i.e. patients that will go on to clinically deteriorate within the first 24 h of clinical presentation, we sought to design and build an innovative POC device to perform the risk prediction at the bedside. Our previously published microfluidic technology^{26,41} was adapted to perform the molecular assay required to quantitate specific mRNAs using ddPCR at POC. The PREDICT system was developed as a stand-alone instrument that integrates the entire automated workflow (Fig. 2A) for detection of the Sepset classifier directly from whole blood—without any pre-processing requirement. The analytical process was split between two microfluidic cartridges that when connected enable RNA isolation and ddPCR biomarker detection (see Methods and Supplementary materials for details including video 1 and video 2) to be performed in sequence automatically. Design of the cartridges and selection of fabrication materials and processes were optimized to ensure compatibility with assay components and reproducible assay execution. Microfluidic cartridges are operated on a centrifugal platform (Fig. 2B)^{26,28,42}. Pneumatically-induced pressure imbalances allowed for transfer, valving, flow switching, inward pumping, and on-demand bubble-based mixing. The combination of centrifugation and pneumatic actuation rendered manipulation of liquids independent of wetting properties, which allowed for automation of the analytical protocol. The sample preparation cartridge (Fig. 2C) contained buffers and reagents (Supplementary Table 6) to isolate RNA from whole blood, which was then used as a template for the ddPCR assay. The detection cartridge was adapted for monodisperse droplet generation and visualization (Fig. 2D–G, Supplementary Table 7).

The analytical workflow was conducted through a timed sequence of centrifugation and pneumatic actuation steps for which operational

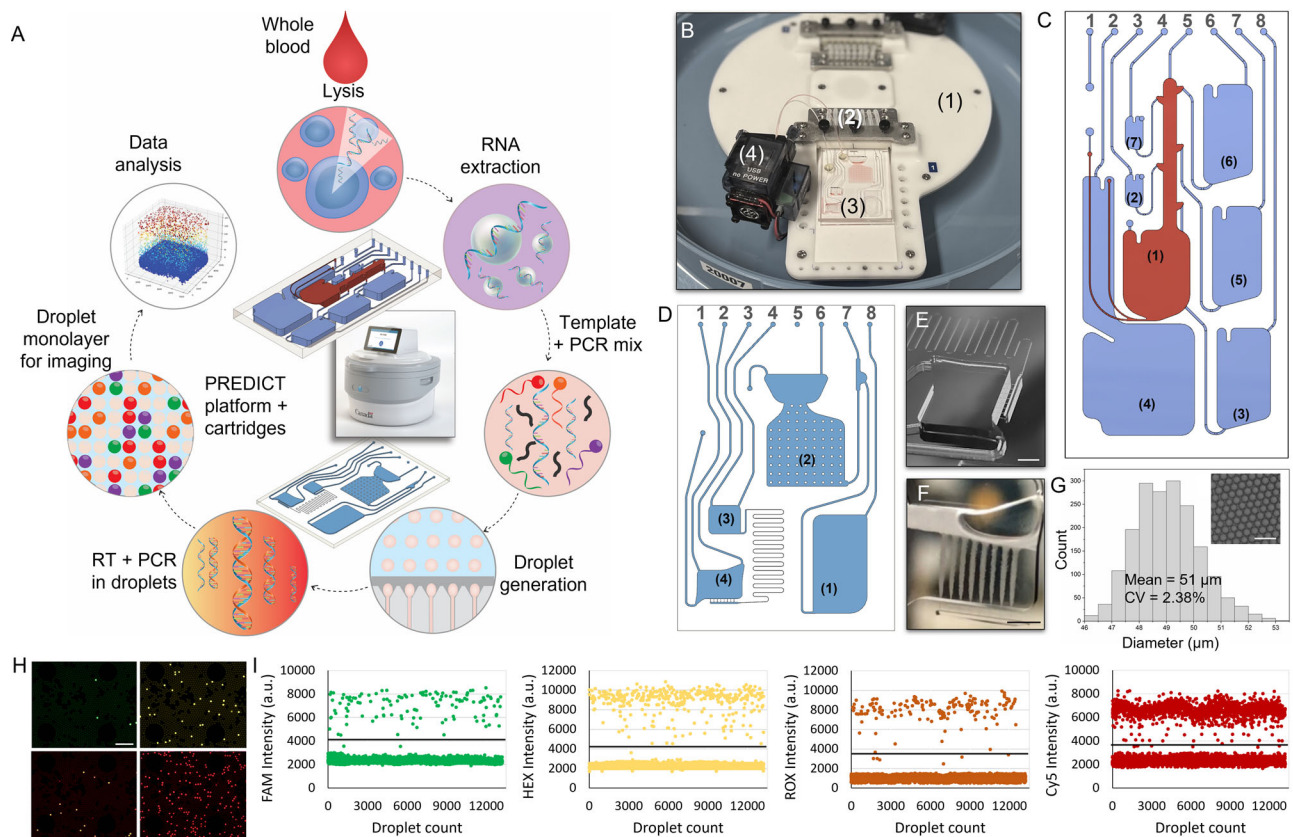


Fig. 2 | Microfluidic platform and cartridges. **A** Microfluidic workflow for automation of RNA extraction and downstream ddPCR on the PREDICT platform and related cartridges. **B** PREDICT platform showing rotor (1), pneumatic manifold (2), cartridge installed on the rotor (3) and connected to the external PCR tube using world-to-chip tubing inserted into the wirelessly controlled platform heater (4). **C** RNA extraction cartridge design. **D** Image of the ddPCR cartridge design. **E** Micrograph showing close-up view of droplet generation chamber and nozzles. The scale bar is 2.4 mm. **F** Micrograph showing close-up view of droplet streams

generated using the ddPCR cartridge. The scale bar is 2.4 mm. **G** Size distribution of droplet diameter. The inset shows optical micrograph of droplet monolayer using ddPCR cartridge. The scale bar is 150 μm . **H** Example of acquired fluorescence images showing droplet monolayer within a region of the imaging chamber. For clarity, only a zoomed-in portion of the imaging chamber region is shown to increase visibility of droplets. The scale bar is 400 μm . **I** Intensity maps for different fluorophores. Horizontal lines denote the threshold for positive and negative counts.

parameters are provided in Supplementary Tables 8 and 9. Supplementary Fig. 5 illustrates the sample preparation and detection cartridges during different stages of the process. The PREDICT system used a miniature epi-fluorescence imaging module for readout of droplets which comprises single-color excitation LEDs and proprietary optical filters for detecting probes labeled with FAM, HEX, ROX and Cy5 fluorophores. The instrument was adapted for recording fluorescence micrographs (Fig. 2H) for each channel in sequence using an embedded monochrome CCD camera equipped with a 2 \times objective that had a sufficiently large field of view (e.g., 8 mm \times 8 mm) to capture >10,000 droplets per image. The proprietary PREDICT software performed image analysis and sample quantification using droplet scatter intensity map for each fluorophore (Fig. 2I) and ‘definetherain’ thresholding algorithm^{43,44}. Comparison of the performance of the PREDICT and BioRad QX200 ddPCR is presented in Supplementary Fig. 6. A proprietary algorithm considered Sepset and HKG expression values and provided results as a probability of clinical deterioration within the next 24 h.

We tested and validated the performance of the PREDICT prototype using label-free real-world samples from clinically annotated patients with prospective sepsis (N = 30, Research Ethics Board # 20-078). These analyses were performed in a blinded fashion using a subset of the 248 technically and clinically benchmarked patients. The PREDICT system was able to predict clinical deterioration at presentation, as determined by worsening of SOFA score or need for ICU admission, providing a risk assessment to physicians regarding the

consequent need for initiation of appropriate therapeutic (antibiotic, anti-viral, immune modulatory and/or monoclonal antibody) or supportive (ICU entry, mechanical ventilation, fluids) measures post-presentation. The sensitivity was 92%, specificity 89%, and overall accuracy 88% (Table 2), consistent with the RT-qPCR assays described above.

Finally, we also looked at how the Sepset classifier compares to lactate in predicting clinical deterioration within 24 h and whether the Sepset signature provided any additional diagnostic value over lactate measurements. We found that a model based on lactate will have poor performance since the lactate level lacked discriminating power between sepsis and non-sepsis cohorts. Lactate is used as a general test for serious health problems, and while used in sepsis, tends to indicate mortality risk⁴⁵, which is separate from progression to sepsis³³. This was confirmed by AUC curves for Hancock ER data which, as expected, showed that the lactate model did not work at all, being no better than a random guess. SepsetER did very well as shown in our manuscript and combining these two parameters actually decreased the AUC (Supplementary Fig. 7).

Discussion

We have demonstrated the successful creation of a predictive sepsis gene expression signature and its migration to a novel POC platform PREDICT as overviewed in the Graphic Abstract (Fig. 3). This proof-of-concept demonstrates the feasibility of developing a rapid POC device that will enable physicians to conduct a prospective sepsis risk

Table 2 | Label-free performance validation of Sepset classifier

RNA-Seq Dataset	AUC	Sensitivity	Specificity	Precision	NPV	Accuracy	Cohorts
RT-qPCR (N = 248)	0.88	94%	72%	84%	88%	83%	This study
ddPCR (N = 30)	0.91	100%	83%	80%	100%	92%	This study
PREDICT (N = 30)	0.88	92%	83%	79%	94%	88%	This study

The PREDICT system was able to predict clinical deterioration at presentation, as determined by worsening of SOFA score or need for ICU admission compared to RT-qPCR and ddPCR. Definitions: RT-qPCR reverse transcription quantitative polymerase chain reaction, ddPCR droplet digital RT-PCR. Supplementary data for this Table is found in Supplementary Data Files 1 and 2.

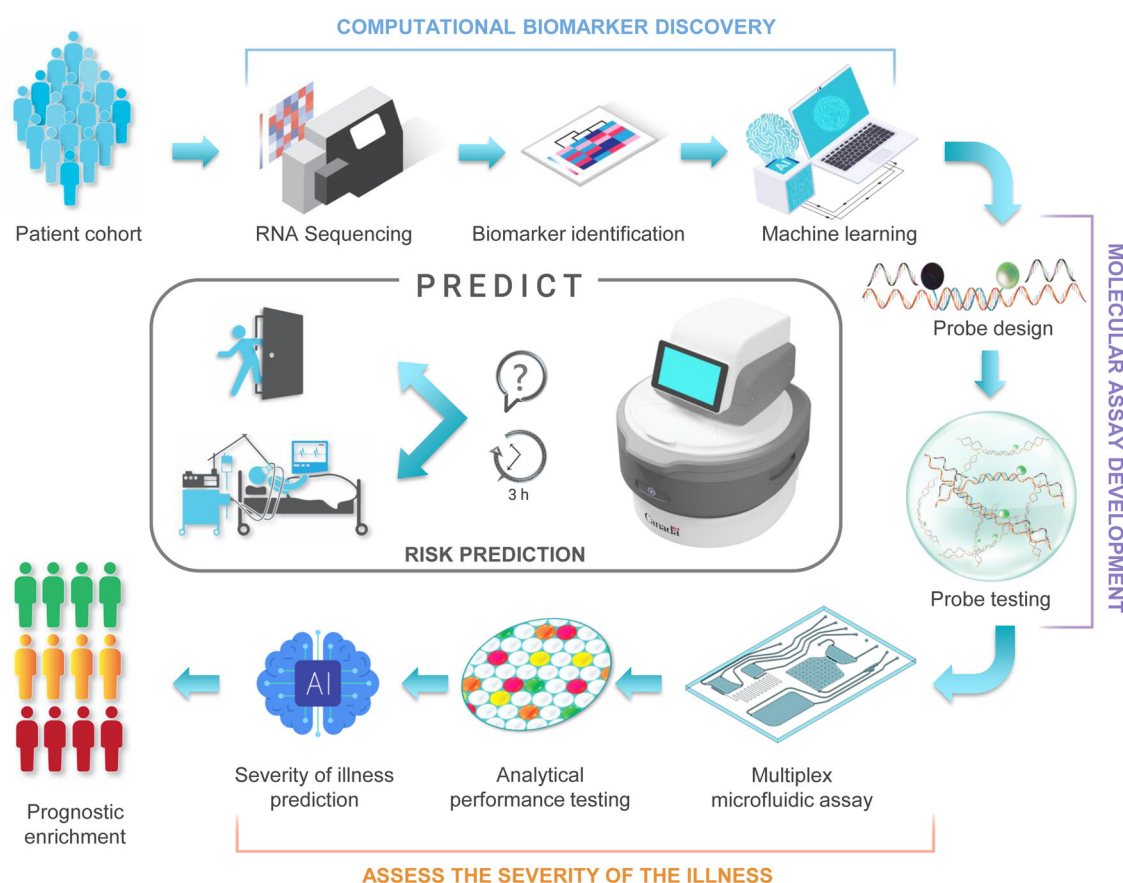


Fig. 3 | Feature reduction and development of a gene classifier that predicts deterioration-risk-groups in patients. This started with taking in-house RNA seq data from patient collected from a heterogenous cohort of patients with suspected sepsis (top left) to reduce our original published gene signature down to 6-genes (Sepset), for which expression could be related to 2 housekeeping genes. Feature selection was performed using machine learning (ML) and AI and the classifier validated in samples from published transcriptomic studies. Molecular assay is then developed by designing and testing primer/probe sequences specific to the target

genes using digital droplet PCR. In parallel, sample-to-answer microfluidic platform and cartridges are developed (bottom right) and analytical performance of multiplex quantitative assay is tested. Prognostic enrichment is obtained by analyzing the results using ML algorithm to determine the percent likelihood of significant clinical deterioration within the immediate next 24 h. The deployment of PREDICT platform (center) at the point-of-care is anticipated to aid in triage and management of prospective sepsis within the first 3 h of clinical presentation.

assessment at the point-of-need (in as little as 1–2 h after clinical presentation). In patients with suspicion of/or early sepsis, a positive result indicates a high probability that the patient will clinically deteriorate in the next 24 h (worsening SOFA score ≥ 2 points and need for ICU admission), guiding physicians as to the need for ICU entry (in ER patients) and interventions like mechanical ventilation. Currently, the device provides a risk assessment in <3 h, well below the 6 ‘golden h’ recommended by the surviving sepsis campaign guidelines¹⁵. In patients with suspected sepsis, PREDICT efficiently performs the entire workflow of RNA signature-based classifier detection, from sample-to-answer using just 50 μ L of whole blood, without requiring pre-preparation of sample, and once transfer of eluate from the first to the second cartridge is automated, with no involvement from the clinical laboratory. Using real-world label-free patient samples, we showed the device has a high sensitivity of 92%, specificity of 89%, and

an overall accuracy of 88% to identify the risk of imminent clinical deterioration in previously benchmarked patients with known outcomes.

There are two other established immune signature-based platforms, but neither appear to be intended for use like the Sepset signature. Septicyte RAPID test⁴⁶, and the original SeptiCyt³⁰, discriminate sepsis from non-infectious systemic inflammation. This test, requires prior sample preparation, including RNA extraction from blood, separates patients into 4 bands with varying accuracy for prediction of sepsis cf. sudden SIRS, with only 55.8% being assigned to the highest and lowest bands and AUCs of 0.81–0.85⁴⁶. In comparative studies, using Sepsis-3 definitions (96% of tested patients had sepsis), the AUC was 0.81, below that for all cohorts with the Sepset signature, except for ER patients not considered in the Septicyte study. Larger (29–31 genes) signatures that predict bacterial vs. viral infections (IMX-BVN3) and sepsis mortality

(IMX-SEV), have been devised and again separate patients into 3 or 4 bands⁴⁷. A recent performance study^{47,48} showed that the IMX-BVN3 signature adjudicated that, amongst patients with confirmed bacterial infections (64% of patients), 31% were possible and 6% were unlikely. Critically, however it is clear that both bacteria and specific viruses like COVID-19 can cause mechanistically almost-identical sepsis, and a positive culture is only found in around 50% of patients^{49–51} even when using the latest molecular detection methods. Thus, discriminating bacterial from viral infections at the host response level may be useful with regards to indicating treatment options but not for identifying sepsis or identifying patients with suspicion of sepsis at risk of clinical deterioration. Conversely the sepsis mortality signature IMX-SEV⁴⁷ shows a good AUC of 0.81 amongst ICU patients but this is separate from the Sepset signature that does not detect eventual mortality (Supplementary Table 4), in contrast to a separate signature we devised³⁶. Overall, Sepset provides a simple binary risk assessment with high accuracy in very large numbers of patients (Table 1).

In our previous study³³ we demonstrated that despite the use of antibiotics in most patients the Sepset signature was robust in determining progression to sepsis. However, in ER patients the sensitivity was lower (70%) than in early ICU patients. It is possible this reflected to some extent that in some ER patients, the early use of antibiotics actually prevented progression to sepsis and organ failure as defined by SOFA score ≥ 2 (74% received antibiotics, Supplementary Table S4). This accuracy increases upon ICU admission suggesting that patients with a positive test or developing symptoms should be retested at a later time (around 6–12 h of hospitalization based on our preliminary analyses), with the likelihood of greater accuracy. We found no statistically significant association of Sepset prediction with presentation systolic or diastolic blood pressure, heart rate, respiratory rate, or temperature, but a modest association with altered mental status (as defined by the Glasgow Coma Scale Score <14 , $p = 0.00099$) and quick SOFA ($p = 0.013$). We found the predictive function of the Sepset signature used in the PREDICT device is independent of initial clinical markers of severity (e.g., presentation lactate), and the association with parameters of deterioration was sustained for up to day 3 (72 h post-presentation) in ICU-admitted patients ($p < 0.005$). These findings strongly suggest the Sepset classifier is not simply detecting a time window of severity; instead, it identifies a specific mechanism-based signature. This signature provides information about immunological cell reprogramming which impairs immune cells' ability to respond to pathogens. This impairment is associated with future clinical deterioration, independent from initial clinical markers of severity. In keeping with this hypothesis, we found that the addition of other clinical or laboratory information, outside of the Sepset classifier, is not required for its performance in predicting which patients are likely to go on deteriorate over the next 24 h. This means that, other than suspicion of sepsis, no other information should be needed for accurate prediction of the clinical course over the first 24 h following initial assessment, although other clinical predictors could complement this test. We have prospectively performed validation of this finding in the COVID cohort that was studied longitudinally³⁹, which suggests that, the PREDICT device may be used in low resource or remote settings, by non-expert personnel, to make immediate risk assessments about level of care.

Currently, there are no universally accepted diagnostic or prediction tools routinely used at the bedside for patients with suspected sepsis; especially during the critical early stages of disease where the risk of clinical deterioration may not be clear. Despite early adequate treatment, many patients fail to improve; highlighting the heterogeneity of the syndrome and the need for pathogen-agnostic risk stratification as well as novel therapeutics^{52–54}. The condition remains misdiagnosed in ~30% of patients⁵⁵. Poor accuracy of current syndromic diagnostic approaches results in unnecessary use of drugs (e.g., antibiotics and steroids) and exposure to harm (iatrogenicity)

associated with hospital and ICU-level care. They also fail to predict, for those patients who are admitted to the ward or are sent home, whether and/or how patients deteriorate and need higher levels of care⁵⁶, placing a considerable financial and human burden on both hospitals and patients, directly affecting prognosis. The primary purpose of the SOFA score is to objectively describe organ (dys)function rather than to predict outcome, so no associated equation developed for prediction is currently in use⁵⁷. There is evidence from a range of observational studies however, that even a small change in SOFA score is associated with a persistent trend in mortality⁵⁸. Recently, Seymour et al.⁵⁹ investigated the validity of the SOFA score to predict in-hospital mortality in patients with suspected infections and found it to have an AUC-ROC of 0.74. Therefore, predicting what the SOFA score will be 24 h post-presentation may have important clinical value. Since SepsetER is based on a gene expression analysis of immunosuppression/cellular reprogramming, there is likely a very strong relationship between a positive (for sepsis) assay and the pathophysiological consequences of a dysfunctional host response to expression as reinforced by the relationship of a positive SepsetER test and organ dysfunction (SOFA score).

Unfortunately, there are important limitations to the calculation and utility of the SOFA score. For example, it requires input from healthcare personnel, and samples need to be processed in a clinical laboratory which may prove challenging when access to clinicians/nurses and/or the laboratory is limited. While a qSOFA has been proposed as a potential solution in low resource settings, there are some intrinsic problems with its utility in guiding early management and qSOFA shows poor accuracy (42–46% in 2 meta analyses^{60,61}). One of the advantages of PREDICT is its potential to provide information about the risk of clinical deterioration independent of the initial SOFA/qSOFA.

The advantages of Sepset and PREDICT include no pre-preparation of the sample, requirement of very small volumes of blood and the accuracy afforded by the use of ddPCR. Importantly, PREDICT is intended for prediction of risk of clinical deterioration in patients suspected of sepsis, so this technology differs fundamentally from most other available tests. Other studies have used retrospective electronic transcriptional data to predict 30-day mortality in adults³¹. The advantage of using a small-sized gene classifier, and the ability to use highly accurate multiplex PCR, needs to be balanced with the need for precision, although we have observed no diminution of effectiveness of the 6 gene signature compared to the 99-gene cellular reprogramming signature from which it was devised³⁴.

An important limitation of our study is that the PREDICT and Sepset classifier are yet to be tested prospectively to determine if its implementation would lead to improved management and outcomes. Although we were able to show high overall accuracy in studies comprising 3178 (all patients in Table 1) or 3426 (Table 1 plus qRT-PCR patients in Table 2) or 3486 (all patients in Tables 1 and 2), there is a paucity of existing cohorts with high-quality (especially RNA-Seq) transcriptomic data for validation, despite the high frequency of sepsis (49 M cases per year). Very few studies have collected early sepsis and/or longitudinal data with accompanying biological samples linked to granular metadata. Since the pandemic, the importance of collecting clinically annotated biological samples for translational research has significantly improved. While showing that we can predict clinical deterioration in patients with bacterial and COVID-19 sepsis, the study should be expanded to other viral causes of sepsis and to important subsets of bacterial sepsis (e.g., caused by particular bacteria). Importantly, we did not have information regarding longer-term outcomes, such as 90-day and hospital mortality for the entire cohort. Our data comes from observational studies, so it precludes us from determining whether the current classifier is informative regarding response to therapy. In contrast, the classifier can be tested in any other cohort even if similar clinical data have not been collected, as

long as clear indicators of clinical deterioration, such as a SOFA scores are available. Given that the PREDICT-based test is conducted in the immediate near-patient environment, the expectation is that there will be no need for storage, transport, or handling of tubes, simplifying its use at the bedside. We have clearly shown that both conventional RT-qPCR and ddPCR as well as the PREDICT platform give very similar accuracy results in all of these three groups. So, we can conclude that the test is quite robust and materials and design have at most a modest impact.

In summary, the current study describes the development of a molecular risk classifier for clinical deterioration and onset of sepsis, and a novel POC device to measure this at the bedside, as well as the proof-of-concept demonstration using real-world patient samples. The important feature of the classifier and the technology is that no additional information, other than suspicion of sepsis, is required to obtain a risk assessment that can be used in a clinically actionable fashion at the bedside. Moreover, in the future, no expert personnel or equipment are required to prepare the sample or interpret the results. Prospective testing of the device and the classifier will be fundamental in moving forward to determine the clinical utility of the tool. However, the technology can be adapted to measure virtually any nucleic acid-based marker, making it modular, and therefore adaptable to easily measure both existing and emerging markers. This adaptability could potentially enhance the predictive performance of the classifier.

Methods

Ethics

This is a multicenter, secondary analysis of a prospectively recruited longitudinal cohort study enrolling consecutive patients with suspected sepsis. All patients were enrolled under local ethical board approval. Informed written consent was obtained upon enrollment from the patient or their legal representative. The Clinical Research Ethics Board (REB) of the University of British Columbia (UBC) provided ethics approval for all sequencing and bioinformatics studies, carried out in a manner blinded to patient identity (approval number REB#H20-02441, REB#H17-01208). Patients recruited and enrolled at Unity Health Toronto were included in accordance with protocol approved by the St. Michael's Hospital ethics board (REB#: 20-078). Patients' data were extracted from the in-hospital electronic medical records, de-identified, and assigned random identification numbers which were used throughout the project. All experiments performed at the NRC involving human samples were approved by the NRC's Ethics Board (NRC REB 2021-57) and experiments were performed according to NRC's policies governing human subjects that follow applicable research guidelines compliant with the laws in the province of Québec.

Sample collection, RNA isolation and cDNA conversion

Patient samples were collected in Pax Gene tubes and total RNA was isolated using standard protocol for Qiagen RNeasy mini kit (#74104). RNA was assessed first using NanoDrop One spectrophotometer (Thermo Scientific) and A260/A280 values were between 1.8 and 2.2, with typical yields in the range of 6–8 µg total. RNA Integrity Number (RIN) was determined using the Agilent 2100 Bioanalyzer (Agilent Technologies). Following the standard Nanochip protocol, samples with RIN values > 7.0 were used for conversion to cDNA. Input volumes for reverse transcription were calculated using the concentration from the bioanalyzer (~500 ng total was used per sample) and a High Capacity cDNA Reverse Transcription Kit (Applied Biosystems #4368814) was used following standard protocols. For RNA-Seq, results have been published³³ including blood collection, RNA extraction and downstream processing. Accession numbers are included in Supplementary Table 1.

Discovery dataset

The whole transcriptome (RNA-seq) data from 586 whole blood samples from different countries and continents comprised our patient cohort. 514 samples were collected and used for discovery analyses (i.e., the discovery cohort). The remaining 72 samples were secondary samples collected from 72 individuals, which were excluded from discovery analyses (to prevent same-individual artifacts) and used as a validation cohort. The sepsis severity associated with the discovery cohort (514) was based on the SOFA score of the patient at 24 h after the first sample collection: 271 samples with SOFA ≥ 2 were sepsis, and 243 samples with SOFA < 2 were non-sepsis.

Sepsis signature and housekeeping gene selection

We tested 99 cellular reprogramming (CR) genes as potential sepsis markers³⁴. We used DESeq2 to perform differential gene expression analyses and chose the genes that had the highest up-regulation (positive fold-change) in high severity samples. We also estimated the predictive accuracy of each CR gene by setting the sensitivity to 75%. We picked six genes (RETN, S100A8, MCEMP1, S100A12, CYP1B1 and HK3) that had the best results in both analyses for the Sepset model.

We analyzed 2833 housekeeping genes³⁸ in our discovery cohort of 514 samples to set a baseline for RNA quantity and sequencing depth. We selected housekeeping genes (HKG) with high and consistent expression across all samples based on mean and variance. We then examined the expression variance of the top 20 HKG candidates across key clinical factors such as age group, gender, sepsis severity, patient location, mortality, etc. The two housekeeping genes (PTP4A2 and CHTOP) with the lowest variances were used to set a baseline for the SepsetER model.

ML algorithm construction and testing

Our own published RNA-Seq data from 873 patient samples³³, was used for feature (gene) reduction using ML. An additional 1241 transcriptomes from patients were used for testing the derived signature. Three major groups of datasets were used for biomarker development – training, validation and testing. The discovery data set (N = 586) was first tested by 10X cross validation and randomly divided into a training (90% of the samples) used for the construction of the models (10,000+ models) and a test dataset (10% of the samples) to assess the best model (Supplementary Fig. 2). We trained 18 different machine learning algorithms on the transcriptomic profiles of the 514 discovery cohort samples. The algorithms were: K-Nearest Neighbors (KNN), Ridge Regression (RR), Lasso regression (LR), Elastic Net (EN), Partial Least Square (PLS), Linear Discriminant Analysis (LDA), Regularized Discriminant Analysis (RDA), Quadratic Discriminant Analysis (QDA), Bayesian Generalized Linear Model (BL), Naïve Bayes (NB), Support Vector Machines (SVM), Decision Tree (DT), Random Forest (RF), Adaptive Boosting (AB), Stochastic Gradient Boosting Model (GBM), Extreme Gradient Boosting (XGB), Neural Network (NN), and Multilayer Perceptron (MLP). We tested each model with different parameters and chose the best one based on the AUC-ROC using 10-fold cross validation, repeated 10 times. We then validated the performance of each model with the additional 72 validation samples (that were not in the training dataset).

We tested the Sepset model with multiple methods. We used various sepsis transcriptome datasets (from microarray and RNA-seq platforms) with over 3000 sepsis and healthy samples to evaluate the SepsetER sepsis classification model. We also trained other published sepsis gene-signatures with our training dataset and compared them with Sepset. The Sepset model, using the Extreme Gradient Boosting (XGB) algorithm, performed better than all other signatures, with a median AUC-ROC of 0.85 in all testing datasets.

Design of primers and probes

The expression of 6 top genes of interest was assessed based on the selection of the highest fold changes with respect to severity of disease in the ICU cohort. These genes (and their amplicon sizes) are HK3 (108 bp), RETN (78 bp), S100A12 (122 bp), S100A8 (122 bp), MCEMP1 (131 bp), CYP1B1 (114 bp). The housekeeping genes were also selected based on stable expression: PTP4A2 (138 bp) and CHTOP (113 bp).

Primers (IDT) for these genes have been designed to span the exon-exon junction to avoid amplification of genomic DNA and to cover the different isoforms. The amplicons' sizes range between 78 bp and 138 bp, as stated above. The probes were synthesized (IDT) with either FAM, HEX, ROX or Cy5 fluorescent labels and a ZEN/3' Iowa Black FQ (IABkFQ) double quencher, when possible, to reduce background noise.

Two fourplex reactions were designed to include 3 genes of interest and 1 HKG for normalization. As such one reaction targeted: CYP1B1, MCEMP1, S100A12 and PTP4A2, and the other: HK3, RETN, S100A8 and CHTOP. The sequences of the primers and probes are provided and described in the supplementary Table 5.

Specificity and sensitivity of the primers and probes were first assessed by performing qPCR standard curves of the individual targeted genes from human universal cDNA (P/N 637223, Clontech/TaKaRa Bio) and comparing the efficiency with the multiplex reaction. The results obtained were then used to design the multiplex ddPCR reactions in order to ensure appropriate amplification of differentially expressed genes and avoid amplification bias.

Commercial duplex ddPCR

For optimal results, recommendations made in the Droplet Digital PCR Applications Guide (Bio-Rad Bulletin 6407) were followed. We used equal concentrations of cDNA for droplet generation following the protocol for ddPCR supermix (Cat # 1863026, Bio-Rad). Briefly, a 22 μ L reaction set-up consists of 2X supermix, 20X probes (a duplex of FAM and HEX), equal concentrations of the patient samples (500 pg), and RNase-free water. The bulk solution (in a 96-well plate) is applied to the AutoDG (automated droplet generator) where the solution is partitioned into 10,000 individual water-in-oil droplets. The 96 well plate is foil sealed and put into the C1000 thermal cycler (Bio-Rad) where the individual droplets are subjected to the following conditions: 10 min at 95 °C, 40 cycles of 30 s at 94 °C and 1 min at 60 °C, followed by 10 min at 98 °C and a 4 °C hold. Subsequently, the droplets were read in the QX200 Droplet Reader using FAM and HEX channel readout in the QuantaSoft software. After data acquisition, the QC of the samples was assessed (ensuring equal droplet numbers generated) and samples were selected in the well selector tool under the Analyze tab. Samples were all manually thresholded using the values from probe alone readout and confirmed in 2D tracings of the duplexed reaction. Samples were tested in duplicate. The concentration reported is "copies/ng DNA" of the final 1X ddPCR reaction.

Microfluidic device fabrication

Sample preparation cartridge. Microfluidic channels and reservoirs were carved into a block (50 mm \times 100 mm \times 6 mm) of Zeonor 1060 R (Zeon Chemicals) using precision machining (Q350 CNC Mill; Menig Automation). The machined polymer piece was cleaned with isopropanol (Sigma-Aldrich) and dried with a stream of nitrogen gas. The microfluidic circuit was sealed using adhesive film (ARclear 93495, 40 μ m in thickness; Adhesive Research) applied on a polycarbonate sheet (#85585K103; 250 μ m in thickness; McMaster-Carr).

Detection cartridge. The microfluidic circuit was fabricated in polydimethylsiloxane (Sylgard 184; Dow Corning) using replica molding. A multi-level SU-8/silicon master mold was made by sequential photolithographic patterning of multiple layers (10, 30 and 50 μ m in thickness) of SU-8 photoresist (GM1060 and GM1070; Gersteltec) spin-

coated onto a 6" silicon wafer (Silicon Quest International) in conjunction with flood exposure at 365 nm (Hg i-line) through a chrome/quartz glass photomask (Photronics) using an EVG 6200 mask alignment system (EV Group). SU-8 resist was developed in propylene glycol monomethyl ether acetate (# 484431 Sigma-Aldrich) for several minutes, followed by rinsing with isopropanol (#19030, Sigma-Aldrich) and drying with a stream of nitrogen gas. Bake steps were performed on a programmable hot plate (HS40A; Torrey Pines Scientific) using recommended time and temperature settings. The liquid pre-polymers of PDMS were mixed at a ratio of 10:1 (w/w) elastomer base/curing agent, poured onto the SU-8/silicon master mold, and cured at 85 °C for 1 h. The cured PDMS replica was bonded to a glass substrate following oxygen plasma activation (HI RF power, 900 mTorr for 30 s; Harrick Plasma).

Microfluidic assay implementation

Total RNA extraction from whole blood. Total RNA was extracted from 50 μ L of whole blood collected in PAXgene tubes using custom Galenvs Total RNA kit (Galenvs) following manufacturer's recommendations. Briefly, whole blood aliquot is mixed with 50 μ L PBS and introduced onto the cartridge for automated protocol or processed manually for extraction in tubes. The mixture was first combined with 20 μ L Proteinase K, and mixed. Lysis/binding buffer was then added to the solution and incubated at 55 °C for 10 min. For manual extraction in tubes, a DynaMag magnetic rack (#12321D Thermo Fisher Scientific) was used to capture magnetic nanoparticles. Following the capture of the RNA bound to the beads, two consecutive wash steps are performed. Elution was performed in 25 μ L of nuclease-free water (Sigma-Aldrich). On-chip extraction of total RNA was performed using the automated protocol (Supplementary Fig. 5A) implemented on the centrifugal platform with the same reagents and volumes as for the manual extraction. For the on-chip capture of magnetic nanoparticles (MNPs), the external magnetic field was provided by a nickel-plated neodymium alloy disk magnet (D201, 1/8" in diameter, 1/32" in thickness; K&J Magnetics) which remained inserted in the designated area on the cartridge for the entire duration of the automated assay. The extracted RNA was assessed using NanoDrop One spectrophotometer and A260/A280 values were between 1.75 and 2.25, with typical yields in the range of 6–7 ng/ μ L for both manual and automated protocols. The extracted RNA was subsequently used in downstream RT-qPCR for assessment of RNA extraction efficiency as well as in on-chip ddPCR for determination of transcript copy number. Ct values for the 8-gene signature were similar for manual and automated extractions (Δ Ct <1) with standard deviation slightly lower for the automated protocol.

qPCR. cDNA obtained from different patients were analyzed in a multiplexed qPCR using primer-probe sequences for genes of interest and housekeeping genes as internal controls for normalization. Each qPCR reaction consisted of 5 μ L 10X PCR Buffer, 8 μ L HotStar Taq Plus DNA Polymerase (Qiagen # 201205), 3 μ L 25 mM MgCl₂, 1 μ L dNTPs, 5 μ L 10X primer-probe mix (final concentration of 1 μ M and 0.5 μ M, respectively), 2 μ L template, and 26 μ L nuclease-free water (Sigma-Aldrich #W4502), for a total volume of 50 μ L. Samples were tested in duplicate. A no-template control (NTC) reaction was included to assess for contamination. Thermal cycling was performed according to the manufacturer's recommended protocol in a Bio-Rad CFX96 Touch Real-Time PCR Detection System (Bio-Rad). To quantify the copies of genes of interest each qPCR run included serial dilutions of cDNA (Takara) generating as such a standard curve. Cq values were plotted against the log concentration and linear regression was used to determine standard curves. The efficiency of each assay was 100 \pm 10% and the R² of each standard curve was >0.98.

RT-ddPCR. The ddPCR reaction master mix comprised of 5 μ L 10X PCR Buffer (#201205, Qiagen), 8 μ L HotStar Taq Plus DNA Polymerase, 8 μ L

100X QuantiTect Virus RT Mix (#211015, Qiagen), 3 μ L 25 mM MgCl₂, 1 μ L dNTPs, 5 μ L 10X primer-probe mix (final concentration of 1 μ M and 0.5 μ M respectively), 2 μ L template, and 18 μ L nuclease-free water (Sigma-Aldrich), for a total volume of 50 μ L. Template input was 2 μ L of cDNA, RNA, or nuclease-free water for NTC samples. On-chip ddPCR assay was performed using an automated protocol implemented on the centrifugal platform (Supplementary Fig. 5B). Briefly, droplets containing template input in ddPCR reaction master mix were generated on-chip in fluorinated carrier oil (5% 00-8 FluoroSurfactant in HFE7500) (RAN Biotechnologies #008-FluoroSurfactant-5wtH-20G). The resultant emulsion was then transferred to the platform heater and cycled following manufacturer's recommended protocol (20 min at 50 °C, followed by 5 min at 95 °C and 40 cycles of 15 s at 95 °C and 45 s at 60 °C, with ramp rate of 1 °C/s). Following thermal cycling, the emulsion was transferred to the chip for fluorescence imaging and data analysis. All experiments were performed in duplicate (no significant differences).

Microfluidic implementation of the SepsetER classifier detection process. The automated RNA extraction protocol (Supplementary Fig. 5A) starts with introduction of the sample in the RNA extraction chamber and installation of the cartridge on the platform. The software then executes a pre-programmed protocol sequence by initiating the platform to rotate. The first step of the automated workflow includes the transfer of a Proteinase K solution to the RNA extraction chamber, and bubble mixing. The lysis/binding buffer containing magnetic nanoparticles is subsequently transferred to the sample, mixed, and incubated for 10 min at 55 °C. The rotation speed is then increased to capture MNPs, and the lysate is transferred to the waste chamber. Two wash steps are then carried out sequentially by transferring the wash solutions from their respective chambers to the RNA extraction chamber. Finally, the purified RNA is eluted in the clean elution buffer.

To begin the cDNA synthesis and ddPCR protocol, a 2 μ L aliquot of the eluted RNA is introduced on the ddPCR cartridge in the PCR mix chamber containing the RT-ddPCR master mix. Two cartridges, each having capacity to perform a single fourplex ddPCR reaction are operated in parallel to detect the 8-gene classifier. The automated sequence (illustrated in Supplementary Fig. 5B) commences by transferring the fluorinated oil into the droplet imaging chamber, followed by emulsification of RT-ddPCR master mix in the droplet generation chamber. The latter is performed by applying a positive pressure onto the ports of the master mix chamber to push the liquid through the resistive serpentine channel entering the array of nozzles connected to the shallow terrace merging into a deep reservoir of the droplet generation chamber. Upon completion of the droplet generation process, the rotation speed is reduced and positive pressure is applied in order to gently transfer the emulsion off-chip into the PCR tube located on the platform heater, using the world-to-chip interface. Following thermal cycling, the emulsion is transferred back on chip by applying positive pressure. The droplets sitting on the top of the oil in the neck of the imaging chamber are subsequently arranged in a monolayer suitable for imaging by applying a low negative pressure at ports of the oil reservoir. This step withdraws (back) the fluorinated oil from the imaging chamber into the oil reservoir and gently lowers the droplets into the shallower portion of the chamber. The pressure is slowly decreased to 0 psi until the monolayer formation is complete and the rotor is stopped, thus allowing the acquisition of fluorescence images for subsequent analysis.

Reporting summary

Further information on research design is available in the Nature Portfolio Reporting Summary linked to this article.

Data availability

Accession codes, unique identifiers, or web links for publicly available datasets are provided in Supplementary Table S1. All data are included in the Supplementary Information or available from the authors, as are unique reagents used in this Article. The raw numbers for charts and graphs are available in the Supplementary Data file 1 and 2.

Code availability

The algorithm has been deposited to Github accession number 963582406 and can be found under the link https://github.com/5dPZ/Diagnostic_assay. The algorithm is provided for academic purposes and copyrighted to restrict unauthorized commercial use.

References

- Singer, M. et al. The Third International consensus definitions for sepsis and septic shock (Sepsis-3). *JAMA* **315**, 801 (2016).
- Reinhart, K. et al. Recognizing sepsis as a global health priority - A WHO resolution. *N. Engl. J. Med* **377**, 414–417 (2017).
- Rudd, K. E. et al. Global, regional, and national sepsis incidence and mortality, 1990–2017: analysis for the Global Burden of Disease Study. *Lancet* **395**, 200–211 (2020).
- Coronavirus (COVID-19). Sepsis Alliance <https://www.sepsis.org/sepsisand/coronavirus-covid-19/>.
- Liu, R., Hunold, K. M., Caterino, J. M. & Zhang, P. Estimating treatment effects for time-to-treatment antibiotic stewardship in sepsis. *Nat. Mach. Intell.* **5**, 421–431 (2023).
- Seymour, C. W. et al. Time to treatment and mortality during mandated emergency care for sepsis. *N. Engl. J. Med* **376**, 2235–2244 (2017).
- Frost, R., Newsham, H., Parmar, S. & Gonzalez-Ruiz, A. Impact of delayed antimicrobial therapy in septic ITU patients. *Crit. Care* **14**, P20 (2010).
- Lo, V. C. K. et al. Management of patients with sepsis in Canadian community emergency departments: a retrospective multicenter observational study. *Health Serv Res Manag Epidemiol* **7**, (2020).
- Bloos, F. & Reinhart, K. Rapid diagnosis of sepsis. *Virulence* **5**, 154–160 (2014).
- van Oers, J. A. H., de Jong, E., Kemperman, H., Girbes, A. R. J. & de Lange, D. W. Diagnostic accuracy of procalcitonin and c-reactive protein is insufficient to predict proven infection: a retrospective cohort study in critically ill patients fulfilling the Sepsis-3 criteria. *J. Appl. Lab Med* **5**, 62–72 (2020).
- Hancock, R. E. W., An, A., dos Santos, C. C. & Lee, A. H. Y. Deciphering sepsis: transforming diagnosis and treatment through systems immunology. *Frontiers Science*, (2025).
- Rudd, K. E. et al. The global burden of sepsis: barriers and potential solutions. *Crit. Care* **22**, 232 (2018).
- Plopper, G. E., Sciarretta, K. L. & Buchman, T. G. Disparities in sepsis outcomes may be attributable to access to care. *Crit. Care Med.* **49**, 1358 (2021).
- Sheikh, F., Douglas, W., Catenacci, V., Machon, C. & Fox-Robichaud, A. E. Social determinants of health associated with the development of sepsis in adults: a scoping review. *Crit. Care Explor* **4**, e0731 (2022).
- Dellinger, R. P. et al. Surviving sepsis campaign: international guidelines for management of severe sepsis and septic shock: 2012. *Crit. Care Med* **41**, 580–637 (2013).
- Asner, S. A., Desgranges, F., Schrijver, I. T. & Calandra, T. Impact of the timeliness of antibiotic therapy on the outcome of patients with sepsis and septic shock. *J. Infect.* **82**, 125–134 (2021).
- Im, Y. et al. Time-to-antibiotics and clinical outcomes in patients with sepsis and septic shock: a prospective nationwide multicenter cohort study. *Crit. Care* **26**, 19 (2022).

18. About WHO. <https://www.who.int/about>.
19. Janasek, D., Franzke, J. & Manz, A. Scaling and the design of miniaturized chemical-analysis systems. *Nature* **442**, 374–380 (2006).
20. Wu, J., Dong, M., Rigatto, C., Liu, Y. & Lin, F. Lab-on-chip technology for chronic disease diagnosis. *npj Digital Med* **1**, 1–11 (2018).
21. Haeberle, S. & Zengerle, R. Microfluidic platforms for lab-on-a-chip applications. *Lab Chip* **7**, 1094–1110 (2007).
22. Mark, D., Haeberle, S., Roth, G., Stetten, F. von. & Zengerle, R. Microfluidic lab-on-a-chip platforms: requirements, characteristics and applications. *Chem. Soc. Rev.* **39**, 1153–1182 (2010).
23. Reddy, B. et al. Point-of-care sensors for the management of sepsis. *Nat. Biomed. Eng.* **2**, 640–648 (2018).
24. Gupta, E. et al. Fast track diagnostic tools for clinical management of sepsis: paradigm shift from conventional to advanced methods. *Diagnostics* **13**, 277 (2023).
25. Oeschger, T., McCloskey, D., Koppa, V., Singh, A. & Erickson, D. Point of Care Technologies for Sepsis Diagnosis and Treatment. *Lab Chip* **19**, 728–737 (2019).
26. Brassard, D. et al. Extraction of nucleic acids from blood: unveiling the potential of active pneumatic pumping in centrifugal microfluidics for integration and automation of sample preparation processes. *Lab Chip* **19**, 1941–1952 (2019).
27. Geissler, M. et al. Centrifugal microfluidic lab-on-a-chip system with automated sample lysis, DNA amplification and microarray hybridization for identification of enterohemorrhagic *Escherichia coli* culture isolates. *Analyst* **145**, 6831–6845 (2020).
28. Malic, L. et al. Automated sample-to-answer centrifugal microfluidic system for rapid molecular diagnostics of SARS-CoV-2. *Lab Chip* **22**, 3157–3171 (2022).
29. Scicluna, B. P. et al. Classification of patients with sepsis according to blood genomic endotype: a prospective cohort study. *Lancet Respir. Med* **5**, 816–826 (2017).
30. McHugh, L. et al. A molecular host response assay to discriminate between sepsis and infection-negative systemic inflammation in critically ill patients: discovery and validation in independent cohorts. *PLOS Med.* **12**, e1001916 (2015).
31. Sweeney, T. E. et al. A community approach to mortality prediction in sepsis via gene expression analysis. *Nat. Commun.* **9**, 694 (2018).
32. Davenport, E. E. et al. Genomic landscape of the individual host response and outcomes in sepsis: a prospective cohort study. *Lancet Respir. Med* **4**, 259–271 (2016).
33. Baghela, A. et al. Predicting sepsis severity at first clinical presentation: The role of endotypes and mechanistic signatures. *EBioMedicine* **75**, 103776 (2022).
34. Pena, O. M. et al. An endotoxin tolerance signature predicts sepsis and organ dysfunction at initial clinical presentation. *EBioMedicine* **1**, 64–71 (2014).
35. Pena, O. M., Pistolic, J., Raj, D., Fjell, C. D. & Hancock, R. E. W. Endotoxin tolerance represents a distinctive state of alternative polarization (M2) in human mononuclear cells. *J. Immunol.* **186**, 7243–7254 (2011).
36. Baghela, A. et al. Predicting severity in COVID-19 disease using sepsis blood gene expression signatures. *Sci. Rep.* **13**, 1247 (2023).
37. An, A. Y. et al. Severe COVID-19 and non-COVID-19 severe sepsis converge transcriptionally after a week in the intensive care unit, indicating common disease mechanisms. *Front. Immunol.* **14**, (2023).
38. Hounkpe, B. W., Chenou, F., de Lima, F. & De Paula, E. V. HRT Atlas v1.0 database: redefining human and mouse housekeeping genes and candidate reference transcripts by mining massive RNA-seq datasets. *Nucleic Acids Res* **49**, D947–D955 (2020).
39. An, A. Y. et al. Post-COVID symptoms are associated with endotypes reflecting poor inflammatory and hemostatic modulation. *Front. Immunol.* **14**, 1243689 (2023).
40. Mammalian Gene Collection | National Institute of Biomedical Imaging and Bioengineering. <https://www.nibib.nih.gov/content/mammalian-gene-collection>.
41. Geissler, M. et al. Centrifugal microfluidic system for colorimetric sample-to-answer detection of viral pathogens. *Lab Chip* **24**, 668–679 (2024).
42. Clime, L., Brassard, D., Geissler, M. & Veres, T. Active pneumatic control of centrifugal microfluidic flows for lab-on-a-chip applications. *Lab Chip* **15**, 2400–2411 (2015).
43. Jones, M. et al. Low copy target detection by Droplet Digital PCR through application of a novel open access bioinformatic pipeline, 'definetherain'. *J. Virological Methods* **202**, 46–53 (2014).
44. Malic, L. et al. Epigenetic subtyping of white blood cells using a thermoplastic elastomer-based microfluidic emulsification device for multiplexed, methylation-specific digital droplet PCR. *Analyst* **144**, 6541–6553 (2019).
45. Bernhard, M. et al. Elevated admission lactate levels in the emergency department are associated with increased 30-day mortality in non-trauma critically ill patients. *Scand. J. Trauma Resusc. Emerg. Med* **28**, 82 (2020).
46. Balk, R. et al. Validation of SeptiCyte RAPID to Discriminate Sepsis from Non-Infectious Systemic Inflammation. *J. Clin. Med* **13**, 1194 (2024).
47. Brakenridge, S. C. et al. Evaluation of a multivalent transcriptomic metric for diagnosing surgical sepsis and estimating mortality among critically ill patients. *JAMA Netw. Open* **5**, e2221520 (2022).
48. Brakenridge, S. et al. The IMX-BVN-3 Classifier detects bacterial infections regardless of anatomical localization in surgical ICU patients (Elsevier Inc., Nashville, TN, 2022).
49. Phua, J. et al. Characteristics and outcomes of culture-negative versus culture-positive severe sepsis. *Crit. Care* **17**, R202 (2013).
50. Tsalik, E. L. et al. Multiplex PCR to diagnose bloodstream infections in patients admitted from the emergency department with sepsis. *J. Clin. Microbiol.* **48**, 26–33 (2010).
51. Nannan Panday, R. S., Lammers, E. M. J., Alam, N. & Nanayakkara, P. W. B. An overview of positive cultures and clinical outcomes in septic patients: a sub-analysis of the Prehospital Antibiotics Against Sepsis (PHANTASI) trial. *Crit. Care* **23**, 182 (2019).
52. Shankar-Hari, M. et al. Reframing sepsis immunobiology for translation: towards informative subtyping and targeted immunomodulatory therapies. *Lancet Respir Med* S2213–2600(23)00468-X (2024) [https://doi.org/10.1016/S2213-2600\(23\)00468-X](https://doi.org/10.1016/S2213-2600(23)00468-X).
53. van der Poll, T., Shankar-Hari, M. & Wiersinga, W. J. The immunology of sepsis. *Immunity* **54**, 2450–2464 (2021).
54. Maslove, D. M. et al. Redefining critical illness. *Nat. Med* **28**, 1141–1148 (2022).
55. Kumar, A. et al. Duration of hypotension before initiation of effective antimicrobial therapy is the critical determinant of survival in human septic shock. *Crit. Care Med* **34**, 1589–1596 (2006).
56. Fernando, S. M. et al. Emergency Department disposition decisions and associated mortality and costs in ICU patients with suspected infection. *Crit. Care* **22**, 172 (2018).
57. Moreno, R. et al. The Sequential Organ Failure Assessment (SOFA) Score: has the time come for an update? *Crit. Care* **27**, 15 (2023).
58. Lambden, S., Laterre, P. F., Levy, M. M. & Francois, B. The SOFA score-development, utility and challenges of accurate assessment in clinical trials. *Crit. Care* **23**, 374 (2019).
59. Seymour, C. W. et al. Assessment of Clinical Criteria for Sepsis: For the Third International Consensus Definitions for Sepsis and Septic Shock (Sepsis-3). *JAMA* **315**, 762 (2016).
60. Jiang, J., Yang, J., Mei, J., Jin, Y. & Lu, Y. Head-to-head comparison of qSOFA and SIRS criteria in predicting the mortality of infected patients in the emergency department: a meta-analysis. *Scand. J. Trauma Resusc. Emerg. Med* **26**, 56 (2018).

61. Wang, C., Xu, R., Zeng, Y., Zhao, Y. & Hu, X. A comparison of qSOFA, SIRS and NEWS in predicting the accuracy of mortality in patients with suspected sepsis: A meta-analysis. *PLoS One* **17**, e0266755 (2022).
62. Burnham, K. L. et al. Shared and Distinct Aspects of the Sepsis Transcriptomic Response to Fecal Peritonitis and Pneumonia. *Am. J. Respir. Crit. Care Med* **196**, 328–339 (2017).
63. Kalantar, K. L. et al. Integrated host-microbe plasma metagenomics for sepsis diagnosis in a prospective cohort of critically ill adults. *Nat. Microbiol* **7**, 1805–1816 (2022).
64. Cani, E. et al. Immunothrombosis biomarkers for distinguishing coronavirus disease 2019 patients from noncoronavirus disease septic patients with pneumonia and for predicting ICU mortality. *Crit. Care Explor* **3**, e0588 (2021).
65. Wang, L. et al. An atlas connecting shared genetic architecture of human diseases and molecular phenotypes provides insight into COVID-19 susceptibility. *medRxiv* 2020.12.20.20248572 (2020) <https://doi.org/10.1101/2020.12.20.20248572>.
66. Tsalik, E. L. et al. Host gene expression classifiers diagnose acute respiratory illness etiology. *Sci. Transl. Med* **8**, 322ra11 (2016).
67. Pankla, R. et al. Genomic transcriptional profiling identifies a candidate blood biomarker signature for the diagnosis of septicemic melioidosis. *Genome Biol.* **10**, R127 (2009).
68. Arunachalam, P. S. et al. Systems biological assessment of immunity to mild versus severe COVID-19 infection in humans. *Science* **369**, 1210–1220 (2020).
69. The Cancer Genome Atlas Program (TCGA) - NCI. <https://www.cancer.gov/ccg/research/genome-sequencing/tcga> (2022).
70. GEO Accession viewer. <https://www.ncbi.nlm.nih.gov/geo/query/acc.cgi?acc=GSE93101>.
71. McCaffrey, T. A. et al. RNA sequencing of blood in coronary artery disease: involvement of regulatory T cell imbalance. *BMC Med. Genomics* **14**, 216 (2021).
72. Arghmann, C. et al. Biopsy and blood-based molecular biomarker of inflammation in IBD. *Gut* **72**, 1271–1287 (2023).
73. Smith, C. L. et al. Identification of a human neonatal immune-metabolic network associated with bacterial infection. *Nat. Commun.* **5**, 4649 (2014).
74. Dapat, C. et al. Gene signature of children with severe respiratory syncytial virus infection. *Pediatr. Res* **89**, 1664–1672 (2021).

Acknowledgements

We acknowledge our membership in the Canadian Critical Care Trials (CCCTG), Canadian Critical Care Translational Biology Group (CCCTBG, CCDS, JM) and Sepsis Canada (RH, JM and CCDS) and are grateful for their insightful review of the manuscript (Drs. A. Fox-Robichaud, and Keith Walley). We are also indebted to Drs. Laurent Brochard, Arthur Slutsky, Amy HY Lee and Gilbert Walker for the insightful comments. We gratefully acknowledge the support from the Canadian Space Agency (CSA) for the development of the PowerBlade hardware system and the digital droplet microfluidic device technology. We further acknowledge funding from the Collaborative R&D Initiative Pandemic Response Challenge Program Grant Application from the National Research Council of Canada to CCDS, RH, TV and LM (2020); the Canadian Institutes of Health Research (CIHR) Collaborative Health Research Projects (CHRP, Natural Sciences and Engineering Research Council of Canada (NSERC) partnered, FDN-433426 to CCDS, TV, LM, MG and DB); CIHR to CCDS (FDN-420463); CIHR to AB and CCDS (Emerging COVID-19 Research Gaps & Priorities, FDN-466806); CIHR COVID-19 Rapid Research Funding and CIHR FDN-154287 to RH. RH holds the University of British Columbia Killam Professorship and previously held a Canada Research Chair. CCDS holds the Robert and Dorothy Pitts Research Chair in Acute and Emergency Medicine and now holds the Tier 1 Canada Research Chair in Accelerated Molecular Translation for Critical Care, and AB holds the Cara Phelan Chair of Critical Care Medicine at the University of Toronto. The COVID cohort studies were

made possible through open sharing of data and samples from the Bio-banque Québécoise COVID-19, funded by the Fonds de recherche du Québec - Santé, Génome Québec and the Public Health Agency of Canada, the University of Toronto COVID Biobank funded by the Canadian Foundation for Innovation (CFI); and the CFI John R. Evans Leaders Fund (CFI-JELF, 2020) and St Michael's Hospital Foundation (2020) for the creation of the PREDICT-biobank at Unity Health Toronto. We thank the research coordinators and biobank managers for their hard work. We especially thank patients and families for their contribution to sepsis research.

Author contributions

LM, LC, CN, DDF, BM, DB, MM, LL, MG and TV were involved in developing the PREDICT point-of-care device and carrying out experiments to test the Sepset algorithm. EEH, RF, MB, and REWH developed the conventional RT-qPCR Sepset test, designed primers, and performed the analyses with this PCR method described in Table 2. PGYZ performed all machine learning studies including extraction of the 6 genes for use in the Sepset test and designing the algorithm for analysis of CT curve results. PP and VS provided initial digital droplet primer design and raw data that was used to optimize the performance of the algorithm. JT and EC performed sample collections and all the RNA extractions for ddPCR used to calibrate algorithm by PP and to benchmark primer performance on the PowerBlade. PP and VS performed the conventional ddPCR analyses described in Table 2. AB, UT, JCM and CCDS supervised all clinical studies. REWH obtained funding for and supervised all studies involved in the development of the Sepset test. CCDS obtained funds and supervised the ddPCR studies and assisted in design of patient-based studies. TV and CCDS co-led the CIHR/NSERC Predict PowerBlade proposal. TV and LM led the development and testing of the PowerBlade prototype development and testing with the NRC team in Boucherville, Quebec (LC, CN, DdF, DB, MM, LL and MG). LM, PGYZ, and PP wrote the first draft of the manuscript, CCDS, TV and REWH wrote the second draft of the manuscript with the assistance of all authors who also read and revised the manuscript.

Competing interests

REWH is an inventor of the Sepset signature that has been patented in 17 countries (e.g. US patent 11,851,717 issued Dec 26, 2023) and is CEO and a shareholder of Asep Medical and its subsidiary Sepset BioSciences Inc. that have licensed in these patents and are actively commercially developing sepsis diagnostics. REWH also has a contract from Sepset Biosciences for development of diagnostic assays for adult sepsis. PGYZ and EFH are employees of Sepset Biosciences Inc. and/or Asep Medical. The PREDICT device is patented e.g. US20170036208A1 with Teodor Veres as a patent holder and assigned to his employer National Research Council of Canada. The remaining authors declare no competing interests.

Additional information

Supplementary information The online version contains supplementary material available at <https://doi.org/10.1038/s41467-025-59227-x>.

Correspondence and requests for materials should be addressed to Claudia C. dos Santos.

Peer review information *Nature Communications* thanks Valeria Garzarelli and the other anonymous reviewer(s) for their contribution to the peer review of this work. A peer review file is available.

Reprints and permissions information is available at <http://www.nature.com/reprints>

Publisher's note Springer Nature remains neutral with regard to jurisdictional claims in published maps and institutional affiliations.

Open Access This article is licensed under a Creative Commons Attribution-NonCommercial-NoDerivatives 4.0 International License, which permits any non-commercial use, sharing, distribution and reproduction in any medium or format, as long as you give appropriate credit to the original author(s) and the source, provide a link to the Creative Commons licence, and indicate if you modified the licensed material. You do not have permission under this licence to share adapted material derived from this article or parts of it. The images or other third party material in this article are included in the article's Creative Commons licence, unless indicated otherwise in a credit line to the material. If material is not included in the article's Creative Commons licence and your intended use is not permitted by statutory regulation or exceeds the permitted use, you will need to obtain permission directly from the copyright holder. To view a copy of this licence, visit <http://creativecommons.org/licenses/by-nc-nd/4.0/>.

© The Author(s) 2025